

# Human Immunodeficiency Virus Type 1 Phylodynamics to Detect and Characterize Active Transmission Clusters in North Carolina

Ann M. Dennis,<sup>1,○</sup> Stéphane Hué,<sup>2,○</sup> Rachael Billock,<sup>3</sup> Sara Levintow,<sup>3</sup> Joseph Sebastian,<sup>4</sup> William C. Miller,<sup>5</sup> and Joseph J. Eron<sup>1,3</sup>

<sup>1</sup>Division of Infectious Diseases, University of North Carolina at Chapel Hill; <sup>2</sup>London School of Hygiene and Tropical Medicine, United Kingdom; <sup>3</sup>Department of Epidemiology, University of North Carolina at Chapel Hill; <sup>4</sup>Campbell University School of Osteopathic Medicine, South Lillington, North Carolina; and <sup>5</sup>Department of Epidemiology, Ohio State University, Columbus

(See the Editorial Commentary by France and Oster, on pages 1223–5.)

**Background.** Human immunodeficiency virus type 1 (HIV-1) phylodynamics can be used to monitor epidemic trends and help target prevention through identification and characterization of transmission clusters.

**Methods.** We analyzed HIV-1 *pol* sequences sampled in North Carolina from 1997 to 2014. Putative clusters were identified using maximum-likelihood trees and dated using Bayesian Markov Chain Monte Carlo inference. Active clusters were defined as clusters including internal nodes from 2009 to 2014. Effective reproductive numbers ( $R_e$ ) were estimated using birth-death models for large clusters that expanded  $\geq 2$ -fold from 2009 to 2014.

**Results.** Of 14 921 persons, 7508 (50%) sequences were identified in 2264 clusters. Only 288 (13%) clusters were active from 2009 to 2014; 37 were large (10–36 members). Compared to smaller clusters, large clusters were increasingly populated by men and younger persons; however, nearly 60% included  $\geq 1$  women. Clusters with  $\geq 3$  members demonstrated assortative mixing by sex, age, and sample region. Of 15 large clusters with  $\geq 2$ -fold expansion, nearly all had  $R_e$  approximately 1 by 2014.

**Conclusions.** Phylodynamics revealed transmission cluster expansion in this densely sampled region and allowed estimates of  $R_e$  to monitor active clusters, showing the propensity for steady, onward propagation. Associations with clustering and cluster characteristics vary by cluster size. Harnessing sequence-derived epidemiologic parameters within routine surveillance could allow refined monitoring of local subepidemics.

**Keywords.** HIV-1; molecular epidemiology; transmission; phylogeny; southeastern United States.

Successful human immunodeficiency virus type 1 (HIV-1) transmission prevention requires targeted approaches tailored to individual epidemics. Molecular epidemiology is increasingly used to reconstruct HIV-1 transmission clusters from viral sequences [1], providing insights into subepidemics overlapping in geography, time, and contact networks. HIV-1 phylodynamic analyses combine viral sequence similarity, molecular clock modeling, and population dynamic inference to reconstruct viral transmission over time [2]. These analyses allow the estimation of transmission parameters among subgroups [3, 4], timing of regional viral introduction [5], and spread [6]. HIV-1 phylodynamics have also been used to identify links between subepidemics [7] and estimate epidemic growth parameters [8, 9], which can inform

public health planning and assessment of interventions [10]. While HIV-1 transmission clusters have been described in multiple cohorts in the United States (US) [11–13], few studies have incorporated phylodynamics [14–16].

Phylodynamic analyses may be particularly informative in regions such as the southern US, where HIV-1 incidence has failed to substantially decline with traditional control measures. Southern states are now an epicenter of the US epidemic [17], with higher HIV-1 diagnosis rates and prevalence compared to other regions. Despite widespread antiretroviral therapy (ART) and advances in prevention, ongoing transmission continues from the prevalent pool of diagnosed and undiagnosed persons living with HIV-1 [18]. As in other southern states, HIV-1 incidence in North Carolina (NC) has not appreciably declined since 2008 [19]; approximately 1400 new HIV-1 diagnoses are reported annually [20]. While our prior studies revealed multiple large clusters composed primarily of men who have sex with men (MSM) [11, 21], sizeable local heterosexual transmission was also identified [21]. Further investigation into HIV-1 clustering dynamics, focusing on growing clusters, is needed to determine optimal approaches for public health response.

Received 25 October 2018; editorial decision 22 February 2019; accepted 11 April 2019; published online April 27, 2019.

Presented in part: 23rd Conference on Retroviruses and Opportunistic Infections, Boston, Massachusetts, February 2016.

Correspondence: A. M. Dennis, MD, 130 Mason Farm Road, Suite 2115, Chapel Hill, NC 27599-6134 (adennis@med.unc.edu).

DOI: 10.1093/infdis/jiz176

We investigated the HIV-1 subtype B transmission dynamics in NC to characterize ongoing transmission networks. We aimed to differentiate between historical and “active” clusters with recent expansion in cluster size, and to estimate temporal parameters and effective reproductive numbers ( $R_e$ ) of active clusters. Delineating demographic and geographic subgroups with high rates of clustering and likely future transmission may inform the design, allocation, and monitoring of combination prevention approaches, such as increased testing and immediate ART [22], allowing for efficient deployment of finite prevention resources.

## METHODS

### Study Population

We analyzed full-length protease (PR, 297 bp) and partial reverse transcriptase (RT, 1200 bp) HIV-1 sequences generated by the Laboratory Corporation of America (LabCorp), the largest commercial laboratory in NC. Sequences were collected from 1997 to mid-2014 from persons accessing clinical care in NC; the majority of the assays were HIV-1 GenoSure. We included samples from patients with a valid date of birth and aged  $\geq 18$  years at the time of sample acquisition. For persons with multiple sequences, only the first available sequence was included. Demographic variables collected included sex and geographic location of sampling sites; diagnosis dates and ART exposure information were not available. Clinic locations were grouped into 1 of the 7 regions used by the NC Department of Public Health to direct HIV-1/STD Field Services (Supplementary Figure 1). This study was approved by the University of North Carolina Institutional Review Board.

### HIV-1 Sequences and Putative Cluster Identification

Sequences were aligned using MUSCLE [23] and manually edited to strip gapped positions. The final sequence length was 1497 bases. Drug resistance mutations (DRMs) were identified using the Stanford HIV-1 Web Service (Sierra version 1.1) to query the Stanford HIV-1db Program [24]. Major DRMs were selected using the 2009 standardized surveillance list from the World Health Organization [25]. Non-B subtype sequences were identified using the Stanford HIV-1db Program and confirmed by the Context-Based Modeling for Expeditious Typing [26] tool as previously described [14].

A maximum-likelihood (ML) phylogenetic tree was constructed in FastTree version 2.1.4 [27] under the general time-reversible model of nucleotide substitution. Statistical support for clades was assessed with local support values (Shimodaira-Hasegawa-like test). Putative transmission clusters were identified using the automated tool ClusterPicker version 1.3 [28]. We defined clusters as clades with high branch support (probability  $\geq 0.90$  by Shimodaira-Hasegawa-like test) and a maximum pairwise genetic distance  $< 3.5\%$  difference between all sequences.

### Time-Scaled Clusters

Subtype B sequences identified in putative clusters in the ML tree were further analyzed using Bayesian Markov Chain Monte Carlo (MCMC) inference in Bayesian Evolutionary Analysis Sampling Trees (BEAST) version 1.8.2 software [29]. Non-B subtypes were evaluated in a separate analysis [14]. Sequences belonging to putative clusters were pooled in batches of  $< 200$  sequences to decrease computational time. Care was taken not to divide clusters between files. Analyses were conducted using the SRD06 nucleotide substitution model, a log-normal relaxed molecular clock model, and the Bayesian skyline model as coalescent tree prior. The MCMC chains were run for 50–100 million generations with 1–5 runs performed for each file. The BEAST log and tree files from multiple runs were combined in LogCombiner version 1.8.2 [29]; 10% of the generations were discarded as burn-in. Convergence of the estimates was considered satisfactory when the effective sample size was  $> 200$ , as calculated in Tracer version 1.6 [30]. Maximum clade credibility trees (MCCTs) were summarized using TreeAnnotator version 1.8.2 [29], keeping the median height over the posterior distribution of trees. Clades with posterior probability  $\geq 0.90$  were considered highly supported.

The time of the most recent common ancestor (tMRCA) of the transmission clusters was estimated as the difference in the sampling date of the most recent sequence in the tree from the median height of the basal node of the cluster identified in the MCCTs. The MCCTs were further assessed for recent subclusters within each cluster. Clusters sized  $\geq 3$  members were considered “active” if the cluster included a recent subcluster, defined as internal nodes with estimated dating in the most recent 5-year sampling period (2009 to mid-2014), and posterior probability  $\geq 0.90$ . Dyads were considered “active” if the median tMRCA was  $\geq 2009$ .

### Identification of Clusters With High Rates of New Sequences, 2009–2014

We examined all clusters that included samples collected 2009–2014. For each year of sampling, a proportional detection rate (PDR) was calculated for each cluster during a given year,  $j$ . We defined this as the cumulative number of clusters members sampled up to and including year  $j$  divided by the cumulative number of cases up to and during the last sampling year ( $i$ ) per observation time between years  $j$  and  $i$ :

$$\text{Proportional Detection Rate (PDR)} = \frac{\sum_0^j \text{Cluster Members}}{\sum_0^i \text{Cluster Members}} \div (j - i)$$

For example, a cluster with samples from 2008 to 2012: one sample each in 2008, 2010, 2011, and then 4 in 2012, would have a PDR = 1 in 2010 ( $2/1 * 1/2$ ), 1.5 in 2011 ( $3/2 * 1/1$ ) and 2.3 in 2012 ( $7/3 * 1/1$ ). For active clusters  $\geq 3$  members in 2009 (baseline), we considered a PDR of  $\geq 2$  (ie, 2-fold increase in size in 1 year) to signify a significant change, which could bring attention to public health authorities for investigation. We evaluated clusters exhibiting a PDR  $\geq 2$  for any year from 2009 to 2014 for clusters reaching size  $\geq 10$  persons by 2014.

### Estimation of Effective Reproductive Numbers

We estimated the  $R_e$  for selected individual large clusters ( $\geq 10$  members) using the birth–death skyline serial (BDSKY) model in BEAST version 2.4.2 [31]. We selected large clusters because BEAST runs become less accurate with smaller clusters sizes and shorter sampling intervals. The BDSKY model infers changes in  $R_e$  over time, thus estimating the average number of new infections caused by an infected person at a specified time during the outbreaks. The  $R_e$  is calculated as the median ratio of the birth and death rates and was estimated for individual clusters over 3 equidistant time dimensions. The 95% highest probability density intervals for  $R_e$  were defined as the smallest intervals containing 95% of the posterior probability of the  $R_e$  estimate [9]. We used a general time-reversible substitution model with a gamma-distributed rate variation and proportion of invariant sites and an uncorrelated log-normal relaxed molecular clock model. The BDSKY model priors were set for  $R_e$  (LogNorm[0;0.5]), the rate of becoming noninfectious (LogNorm[1.3;1]), sampling rate (Beta[10;10]), and a fixed substitution rate of  $3 \times 10^{-3}$  nucleotide substitutions per site per year [32]. We estimated our sampling fraction as approximately 50% based on state surveillance reports that 28 101 HIV-1 cases are currently alive and residing in the state among 42 889 cases reported in NC from 1983 to 2013 [33]. Convergence was considered satisfactory when effective sample size was  $>200$  for relevant parameters.

### Statistical Analyses

We assessed cluster characteristics by cluster size. Dynamics of male-dominated (defined as  $>50\%$  male members) clusters were compared to large clusters composed of  $\geq 50\%$  female members. All descriptive analyses were conducted using Stata version 13.0 software (StataCorp). We calculated assortativity coefficients for sex, age, and sampling region among persons sampled during 2009–2014 identified in active clusters using the *igraph* package in R.

## RESULTS

### Study Population

A total of 15 246 individuals aged  $\geq 18$  years at the time of initial sample collection provided 24 972 HIV-1 *pol* sequences. Of these persons, 14 921 (97.9%) had subtype B sequences ( $n = 24\ 511$  sequences) and were included in further analyses. Most persons ( $n = 9973$  [67%]) had only 1 available sequence. Among persons with subtype B samples, 10 550 (70.7%) were male and 4173 (28.3%) were female (Table 1). The median year of the first available sequences was 2008 (interquartile range [IQR], 2005–2011) and the median age of sampled persons at the time of the first available sequence was 40 (IQR, 32–48) years. Most sequences ( $n = 10\ 143$  [68.0%]) were sent from clinics in the Raleigh or Charlotte regions, the most populous regions in the state (Supplementary Figure 1).

**Table 1. Comparison of Characteristics of Human Immunodeficiency Virus Type 1–Infected Individuals and Their First Available Subtype B *pol* Sequences Sampled in North Carolina From 1997 to 2014, by Cluster Inclusion and Cluster Size**

Characteristic	Total (N = 14 921)		Not in Cluster (n = 7413)		In Cluster (n = 7508)					
					2 Members (n = 2452)		3–9 Members (n = 3994)		10–36 Members (n = 1062)	
	No.	(%)	No.	(%)	No.	(%)	No.	(%)	No.	(%)
Sex (n = 14 732)										
Male	10 550	(71.7)	5169	(71.0)	1651	(68.0)	2882	(72.8)	848	(80.6)
Female	4173	(28.3)	2115	(29.0)	776	(32.0)	1078	(27.2)	204	(19.4)
Age, y										
$\geq 35$	10 107	(67.7)	5670	(76.5)	1706	(69.6)	2304	(57.7)	427	(40.2)
$< 35$	4814	(32.3)	1743	(23.5)	746	(30.4)	1690	(42.3)	635	(59.8)
Sample year										
2009–2014	6874	(46.1)	3000	(40.5)	1066	(43.5)	2120	(53.1)	688	(64.8)
2003–2008	5993	(40.2)	3077	(41.5)	1046	(42.7)	1528	(38.3)	342	(32.2)
1997–2002	2054	(13.8)	1336	(18.0)	340	(13.9)	346	(8.7)	32	(3.0)
Region of sampling										
1 – Asheville/Western	727	(4.9)	385	(5.2)	145	(5.9)	172	(4.3)	25	(2.4)
2 – Charlotte	3776	(25.3)	1856	(25.0)	634	(25.9)	1052	(26.3)	234	(22.0)
3 – Winston-Salem	1069	(7.2)	612	(8.3)	163	(6.7)	258	(6.5)	36	(3.4)
4 – Raleigh	6367	(42.7)	3054	(41.2)	1013	(41.3)	1724	(43.2)	576	(54.2)
5 – Fayetteville	1174	(7.9)	547	(7.4)	196	(8.0)	324	(8.1)	107	(10.1)
6 – Greenville	1066	(7.1)	585	(7.9)	158	(6.4)	296	(7.4)	27	(2.5)
7 – Wilmington	742	(5.0)	374	(5.1)	143	(5.8)	168	(4.2)	57	(5.4)

### Characteristics of Transmission Clusters

From the initial ML tree, 2283 putative transmission clusters were identified among the 14 921 subtype B sequences from unique individuals. These clusters included 7560 (50.7%) individuals. Only 52 (0.7%) sequences identified in the putative ML clusters were not in clusters with posterior probability >0.9 ( $n = 29$  clusters) in the BEAST analysis. Nine of the ML clusters (34 persons) were broken down into 10 smaller clusters in the BEAST analysis (24 persons) with high posterior probability support; the remaining 10 persons were considered not clustered. Another 20 BEAST clusters had low posterior probability support (all 2–3 members) and were excluded (42 persons). The final BEAST trees included 7508 (50.3%) sequences in 2264 clusters with posterior probability >0.9. We identified 1227 dyads (54.2%), 963 clusters of 3–9 persons (42.5%), and 74 (3.2%), large clusters ( $\geq 10$  members); median cluster size was 2 (IQR, 2–4) members (Supplementary Table 1).

Characteristics of nonclustered persons differed substantially from characteristics of those identified in BEAST clusters (Table 1). A similar proportion of nonclustered persons and persons in dyads were male (71.0% vs 68.0%), compared to 80.6% of persons in large clusters. A large proportion of those not in clusters (76.5%) were  $\geq 35$  years of age at the time of sequencing, while the proportion of those <35 years of age increased with cluster size. Nonclustered individuals also tended to have earlier sequence sampling years than those in clusters.

### Phylodynamics and Detection of Active Clusters

The vast majority of clusters of all sizes had estimated tMRCA dated prior to 2010; just 5.7% of dyads and 1.1% of clusters of 3–9 members had estimated tMRCA dates between 2010 and 2014. All large clusters had a tMRCA estimated before 2010. Of the 74 large clusters ( $\geq 10$  members), 58 (78.4%) were male-dominated (>50% male members) and 16 (21.6%) were composed of  $\geq 50\%$  female members (Figure 1). Male-dominated

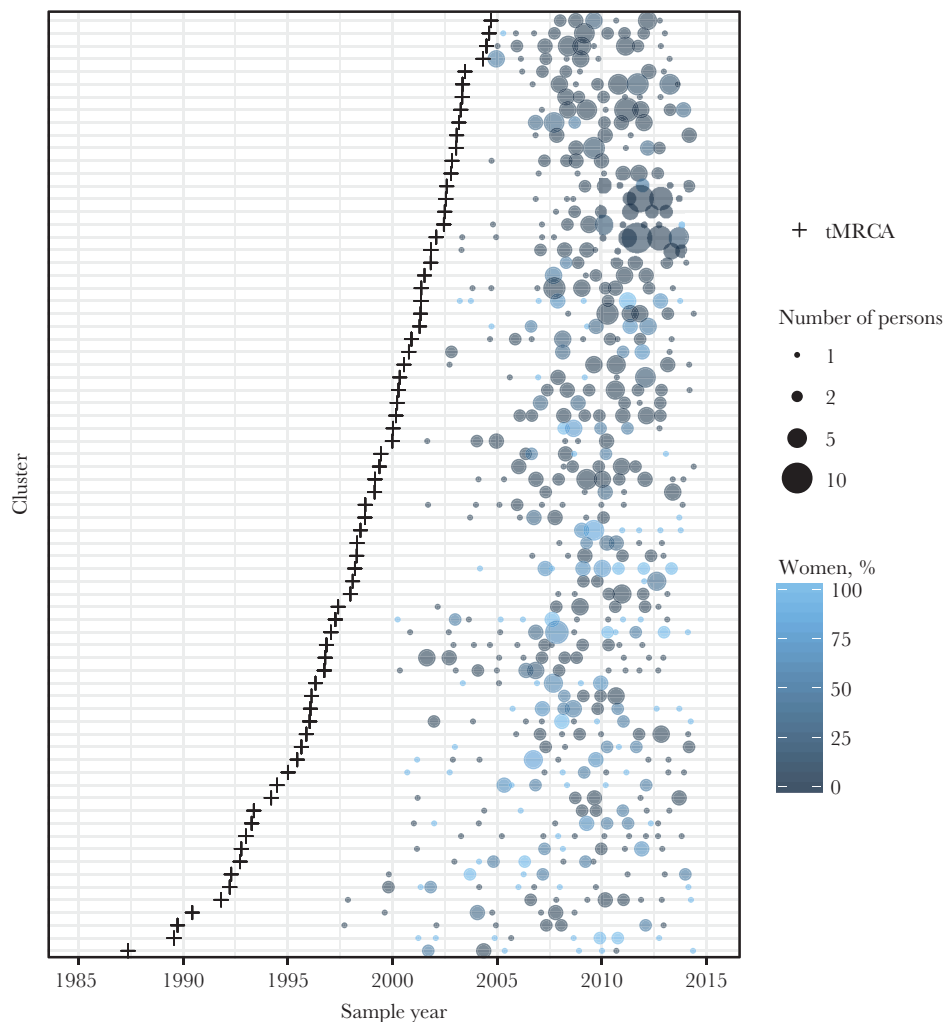


**Figure 1.** Distribution of large clusters ( $\geq 10$  members;  $n = 74$  clusters) among 2264 subtype B clusters identified among 14 921 persons with HIV-1 *pol* sequences sampled, 1997–2014. Each cluster is a horizontal line on the y-axis. The x-axis indicates the number of samples (only the first per person) by sampling year. The cross (+) indicates the time of the most recent common ancestor (tMRCA) of the cluster, as estimated in BEAST version 1.8. Color gradient indicates the percentage of samples in each cluster per year from women.

and  $\geq 50\%$  female clusters had similar median cluster sizes (13 [IQR, 11–17] vs 13 [IQR, 10–15] members). Male-dominated clusters had more recent introduction (median year of tMRCA: 1999 [IQR, 1995–2002] vs 1996 [IQR, 1993–1997]) and shorter time spans (15 years [IQR, 12–19] vs 18 years [IQR, 16–19] compared to clusters  $\geq 50\%$  female).

We assessed recent subclusters within each cluster defined as a highly supported internal node dated between 2009 and 2014, the most recent sampling period. The median year of the most recent internal node among clusters was 2003.5 (IQR, 1984.6–2007.3). In total, 12.7% clusters (288/2264) had recent nodes from 2009 to 2014. Of the 10 largest clusters ( $\geq 20$  members), 8 (80%) had recent subclusters, indicating relatively recent cluster expansion. Clusters with a recent internal node were defined as active clusters.

#### Cluster Composition and Assortativity of Active Clusters 2009–2014

Of 2264 clusters, 1639 (72%) contained at least 1 sequence sampled between 2009 and 2014. However, more than two-thirds ( $n = 1351$  [68%]) of these clusters were more likely to be historical, containing no internal nodes after 2008. Cluster characteristics associated with these active and historical clusters were evaluated. As expected, active clusters compared

to historical clusters are larger (63% vs 47% have 3–9 members and 12.9% vs 2.7% have  $\geq 10$  members), contain more younger persons (37% vs 14% are composed of  $>50\%$  persons under 30 years), and are majority male (73% vs 58%) ([Supplementary Table 2](#)).

We assessed the sex and age distributions of the 288 active clusters and evaluated rates of detection of additional new sequences in the 2009–2014 sampling period. Cluster composition differed substantially by cluster size among the 288 active clusters ([Tables 2 and 3](#)). More than half of dyads (52.9%) contained at least 1 woman, while larger clusters were dominated by men. Overall, 51% of clusters (147/288) contained only men. However, nearly half of clusters (49%) involved women. Among the 1306 persons in these 288 active clusters, the assortativity coefficient  $r$  was 0.37 for sex, 0.43 for age, and 0.47 for sampling region, indicating assortative mixing of these characteristics ( $r = 1$  indicates perfect assortativity). However, assortativity differed by cluster size, where dyads were nonassortative by sex ( $r = -0.08$ ) ([Table 2](#)).

#### Large Clusters With High PDR, 2009–2014

Among all active clusters ( $n = 288$ ), there were 110 (38.2%) that more than doubled in size in 1 year from 2009 to 2014 ( $\text{PDR} \geq 2/$

**Table 2. Characteristics of 288 “Active” Clusters That Involve Recent Internal Nodes (2009–2014), by Cluster Size**

Cluster Characteristic	Cluster Size					
	2 Members ( $n = 70$ )		3–9 Members ( $n = 181$ )		10–36 Members ( $n = 37$ )	
<b>Sex</b>						
$\geq 50\%$ female	37	(52.9)	36	(19.9)	5	(13.5)
$>50\%$ male	33	(47.1)	145	(80.1)	32	(86.5)
<b>Female members</b>						
0	33	(47.1)	99	(54.7)	15	(40.5)
$\geq 1$	37	(52.9)	82	(45.3)	22	(59.50)
<b>Male members</b>						
0	5	(7.1)	3	(1.7)	0	(0)
$\geq 1$	65	(92.9)	178	(98.3)	37	(100)
<b>Age <math>&lt;30</math> y (<math>&gt;50\%</math>)</b>						
Yes	13	(18.6)	72	(39.8)	21	(56.8)
No	57	(81.4)	109	(60.2)	16	(43.2)
<b>Cluster detection, 2009–2014</b>						
New	70	(100)	86	(47.5)	3	(8.1)
Expanding	0	(0)	95	(52.5)	34	(92)
<b>Cluster size in 2009, median (IQR)</b>						
	0	(0)	1	(0–1)	4	(2–5)
<b>Sequences 2009–2014, median (IQR)</b>						
	2	(2–2)	4	(3–5)	11	(9–13)
<b>Rate cluster size increase<sup>a</sup></b>						
	...	...	2	(1.5–2.5)	3.5	(1.5–7)
<b>tMRCA, median year (IQR)</b>						
	2010	(2010–2011)	2002	(1999–2006)	2001	(1998–2003)
<b>Cluster time span, y, median (IQR)</b>						
	2.1	(1.3–2.9)	10.8	(7.6–13.8)	13.1	(11.3–15.6)
<b>Assortativity coefficient</b>						
Sex	–0.08		0.36		0.37	
Age	0.72		0.46		0.37	
Region of sampling	0.65		0.44		0.48	

Data are presented as No. (%) unless otherwise indicated.

Abbreviations: IQR, interquartile range; tMRCA, time of the most recent common ancestor.

<sup>a</sup>Rate increase during 2009–2014 for expanding clusters. Calculated as number of new sequences detected in clusters 2009–2014 / size baseline cluster (in 2009).

**Table 3. Characteristics of Persons With First Sample in 2009–2014 Who Are Members of Active Clusters**

Characteristic	Cluster Size					
	2 Members (n = 140)		3–9 Members (n = 737)		10–36 Members (n = 429)	
	No.	(%)	No.	(%)	No.	(%)
<b>Sex (n = 1300)</b>						
Male	98	(70.5)	590	(80.4)	370	(86.7)
Female	41	(29.5)	144	(19.6)	57	(13.4)
<b>Age, y</b>						
<35	62	(44.3)	443	(60.1)	301	(70.2)
>35	78	(55.7)	294	(39.9)	128	(29.8)
<b>Region of sampling</b>						
2 – Charlotte	39	(27.9)	196	(26.6)	102	(23.8)
4 – Raleigh	54	(38.6)	302	(40.9)	231	(53.9)

year). Of these, 27 of 110 (24.6%) were dyads, 68 of 110 (62.8%) contained 3–9 members, and 15 of 110 (13.6%) contained 10–36 members by 2014. For active clusters, the median PDR was 1.25 (IQR, 0.83–1.6) per year compared to historical clusters where the median was lower at 0.75 (IQR, 0.4–1.3) per year.

Of the 15 clusters with high PDR, and size  $\geq 10$  members by 2014, all were male dominated (Figure 2A). Large, high PDR clusters averaged 1.5 members (range, 0–5) at baseline (2009) and the mean maximum PDR per cluster was 2.7 per year. All of these clusters originated before 2007 and most were homogeneous by sampling region (Figure 2B).  $R_c$  estimates for these clusters rarely fell below 1 and generally remained stable around 1 with occasional fluctuations (Supplementary Figure 3). The median  $R_c$  was around 1 for most clusters for the most recent time interval (Figure 2A), which spanned an average of 3 years (from 2011 to 2014). One large cluster (Cluster ID 1076) had an increasing  $R_c$  over the 3 time intervals, with the latest interval estimated at 1.66 (95% highest probability density, 1.03–2.50) (Figure 3A). Conversely, another cluster (Cluster ID 618) had a decreased  $R_c$  (Figure 3B). The mean sampling proportion estimated by the birth–death model was 0.47 on average across the clusters; this is consistent with our estimated sampling of 50% based on NC surveillance reports.

#### Large Clusters With Low PDR, 2009–2014

For further comparison of the birth–death model, we estimated the  $R_c$  over time for the 5 largest clusters ( $n \geq 20$  members) with low PDR from 2009–2014. For all of these clusters, the  $R_c$  declined in the third estimation time frame (Supplementary Figure 4).

## DISCUSSION

We used a large statewide repository of HIV-1 sequence data with sampling extending over 15 years to identify ongoing HIV-1 transmission networks defined by phylogenetic clustering. We found a high degree of clustering indicating significant local onward transmission. Applying time-scaled

analyses, we provide a framework to identify clusters that are active and estimate basic epidemiologic parameters from these clusters, which could be used for epidemic monitoring. Most large clusters examined may continue to propagate at a steady pace. Future work to incorporate such large-scale sequence and phylodynamic analyses with traditional HIV-1 surveillance (ie, partner notification networks, risk behaviors) may help monitor the effect of interventions and direct allocation of public health resources.

We employed molecular clock analyses to estimate origins and time spans for individual clusters, revealing that the HIV-1 transmission dynamics of male-dominated clusters differed compared to clusters including at least half women. Overrepresentation of women in dyads and men in clusters likely reflects that local transmission is dominated by MSM. Male-dominated clusters originated more recently and tended to have shorter time spans. Furthermore, our prior analyses among clinic cohort participants failed to reveal any large clusters dominated by persons who inject drugs [11, 21]. Thus, we expect that the vast majority of clusters including women involve heterosexual transmission. Dynamics of heterosexual vs MSM transmission have been shown to differ substantially and similarly to our observations in other settings. In the United Kingdom, smaller clusters and slower transmission dynamics were found among heterosexual individuals compared to MSM [4]. However, our study reveals larger heterosexual clusters compared to those in European cohorts, likely reflecting mixed transmission dynamics in the US Southeast.

While characteristics associated with cluster membership, such as male sex and younger age, parallel incidence trends in the region [20], phylodynamic data offer important insights into local transmission dynamics not ascertainable through traditional surveillance. Phylodynamic trends lend information on the degree of localized transmission within the region, giving estimates on cluster origins and time spans. Although most large clusters analyzed in this study originated over a decade before the end of the study period, a large proportion

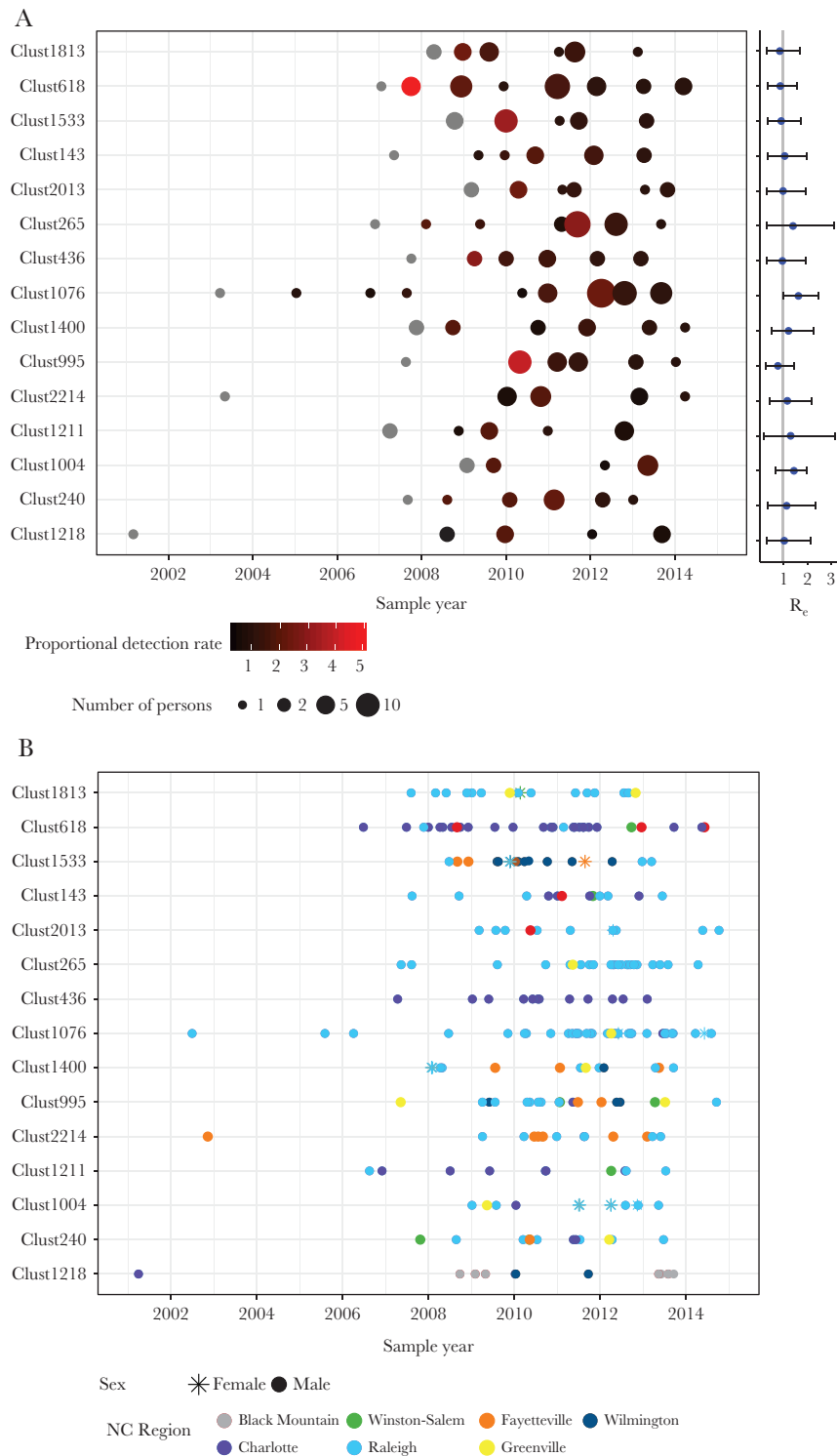


**Figure 2.** Distribution of clusters with high proportional detection rate (PDR) ( $\geq 2$ -fold increase in cluster size) between 2009 and 2014 and size  $\geq 10$  members by 2014 ( $n = 15$  clusters). The y-axis indicates cluster identification number. *A*, Number of samples per year. Color gradient indicates PDR. The effective reproductive number ( $R_e$ ) and 95% credibility intervals estimated in the most recent time span (~2011–2014) is indicated for each cluster. *B*, Number of samples per year, by North Carolina (NC) region of sampling and sex.

had increased in size since 2009. Much of this growth was observed among young men. However, more than half of these clusters also include women. Ongoing heterosexual

transmission in these clusters may be fueled by men who have sex with men and women [34], although no behavioral data were available in our study. Nonetheless, this finding

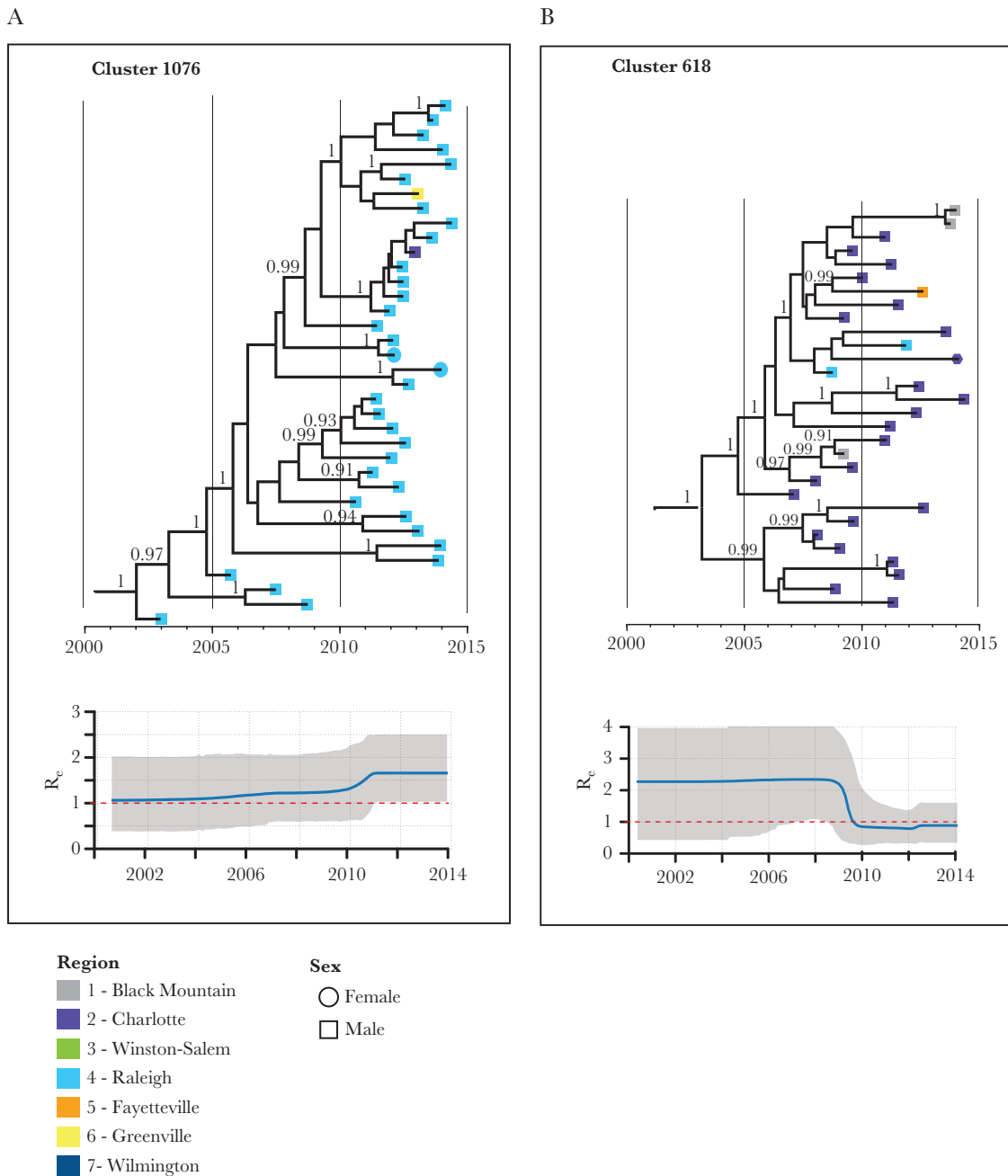


**Figure 3.** Effective reproductive number ( $R_e$ ) and section of maximum clade credibility tree among selected clusters with size  $\geq 10$  members by 2014 and high proportional detection rate from 2009 to 2014. Clades with posterior probability  $\geq 0.90$  are labeled. *A*, Cluster 1076 with increasing  $R_e$  and majority samples from the Raleigh region. *B*, Cluster 618, with  $R_e$  trending downward and sampling from multiple North Carolina regions.

emphasizes the importance of continued prevention efforts to help identify high-risk women.

We estimated the reproductive numbers of clusters based on HIV-1 sequence data, showing that many large clusters are propagating at a steady pace as of 2014. An  $R_e$  around 1 implies no significant epidemic expansion—or decline. This is consistent with a growing number of prevalent cases. The stability of the epidemic size model, applies to the number of infected persons not on ART (largely undiagnosed) because in

the model, persons are considered “removed” after sampling. A study in Botswana [8] similarly estimated  $R_e$  though among subtype C clusters ( $\geq 5$  members; median  $R_e$  ranged from 0.72 to 1.77), suggesting that  $R_e$  trends could be used to prioritize clusters for targeted interventions. The trend in  $R_e$  over time may be most useful in monitoring the effect of existing prevention efforts or interventions on cluster growth. Of note, estimated  $R_e$  scores rely on both the potential for clusters to produce new infections and the likelihood that these infections



are detected and sequenced. Thus, clusters with poor sampling rates may show downwardly biased  $R_c$  values.

A strength of this study is the likely large sampling density compared to prior phylogenetic studies conducted in the US, which minimizes sampling bias that can affect clustering interpretations [34]. Nonetheless, our observations could be influenced by differential sampling, particularly among subpopulations or within geographic regions. We defined active clusters as those with a highly supported subcluster in the most recent 5-year sampling period. Thus, incomplete sampling could underestimate the number of active clusters. Other factors associated with clustering, such as more recent sampling year and younger age, could be due to these groups being more likely to have a sequence. Other analytical approaches, such as source attribution methods, are less susceptible to sampling bias [35], and more work needs to be done to compare results with phylogenetic clustering.

Integration of epidemiological information would allow estimation of HIV-1 transmission sources and improved identification of potential intervention targets based on molecular analyses. We found positive—but not perfect—assortativity by sex, age, and region among large clusters; thus, many include exchange across these subgroups, which can inform how cluster-directed interventions are planned. Our analyses are limited by lack of information on diagnosis dates, infection duration prior to sequencing, ART exposure, RNA viral loads, and risk behaviors. We were also only able to include viral sequences processed by a single reference laboratory in NC.

The Centers for Disease Control and Prevention have expanded its program to evaluate HIV-1 molecular clusters nationwide based on sequences reported through surveillance in many state health departments [36]. While HIV-1 phylogenetics have historically focused on retrospective datasets, these analyses can help plan and assess interventions [10, 37]. Such interventions include intense allocation of immediate ART, preexposure prophylaxis, and increased testing toward active clusters. By assessing sources of transmission among recently infected MSM in the Netherlands, one study found that the majority of recent infections could have been prevented with a combination approach informed by phylogenetic analyses [22].

We are currently developing an automated sequence analysis tool integrated with surveillance data to assess HIV-1 genetic clustering in NC to provide near real-time, actionable insight into HIV-1 transmission dynamics for the development of public health interventions. Reducing HIV-1 incidence requires earlier diagnosis, effective care linkage, and retention in care to achieve longstanding viral suppression. Allocating intense interventions toward clusters with high potential for further onward transmission demonstrated by increasing  $R_c$  could more effectively reduce HIV-1 incidence than traditional methods. Application of phylodynamic methods within the surveillance system will inform the timely development and monitoring of

public health interventions and HIV-1 transmission trends in NC with methods translatable to other settings.

### Supplementary Data

Supplementary materials are available at *The Journal of Infectious Diseases* online. Consisting of data provided by the authors to benefit the reader, the posted materials are not copyedited and are the sole responsibility of the authors, so questions or comments should be addressed to the corresponding author.

### Notes

**Disclaimer.** The content is solely the responsibility of the authors and does not necessarily represent the official views of the National Institutes of Health (NIH).

**Financial support.** This work was supported by the National Institute of Allergy and Infectious Diseases, NIH (grant number K08AI112432-01) and by the University of North Carolina Center for AIDS Research (grant number P30AI50410).

**Potential conflicts of interest.** All authors: No reported conflicts of interest. All authors have submitted the ICMJE Form for Disclosure of Potential Conflicts of Interest. Conflicts that the editors consider relevant to the content of the manuscript have been disclosed.

### References

1. Hassan AS, Pybus OG, Sanders EJ, Albert J, Esbjörnsson J. Defining HIV-1 transmission clusters based on sequence data. *AIDS* **2017**; 31:1211–22.
2. Volz EM, Koelle K, Bedford T. Viral phylodynamics. *PLoS Comput Biol* **2013**; 9:e1002947.
3. Lewis F, Hughes GJ, Rambaut A, Pozniak A, Leigh Brown AJ. Episodic sexual transmission of HIV revealed by molecular phylodynamics. *PLoS Med* **2008**; 5:e50.
4. Hughes GJ, Fearnhill E, Dunn D, et al. Molecular phylodynamics of the heterosexual HIV epidemic in the United Kingdom. *PLoS Pathog* **2009**; 5:e1000590.
5. Gray RR, Tatem AJ, Lamers S, et al. Spatial phylodynamics of HIV-1 epidemic emergence in East Africa. *AIDS* **2009**; 23:F9–17.
6. Magiorkinis G, Angelis K, Mamais I, et al; SPREAD Program. The global spread of HIV-1 subtype B epidemic. *Infect Genet Evol* **2016**; 46:169–79.
7. Skar H, Axelsson M, Berggren I, et al. Dynamics of two separate but linked HIV-1 CRF01\_AE outbreaks among injection drug users in Stockholm, Sweden, and Helsinki, Finland. *J Virol* **2011**; 85:510–8.
8. Novitsky V, Kühnert D, Moyo S, Widenfelt E, Okui L, Essex M. Phylodynamic analysis of HIV sub-epidemics in Mochudi, Botswana. *Epidemics* **2015**; 13:44–55.
9. Stadler T, Kouyos R, von Wyl V, et al. Estimating the basic reproductive number from viral sequence data. *Mol Biol Evol* **2012**; 29:347–57.

10. Paraskevis D, Nikolopoulos GK, Magiorkinis G, Hodges-Mameletzis I, Hatzakis A. The application of HIV molecular epidemiology to public health. *Infect Genet Evol* **2016**; 46:159–68.
11. Dennis AM, Hué S, Hurt CB, et al. Phylogenetic insights into regional HIV transmission. *AIDS* **2012**; 26:1813–22.
12. Aldous JL, Pong SK, Poon A, et al. Characterizing HIV transmission networks across the United States. *Clin Infect Dis* **2012**; 55:1135–43.
13. Little SJ, Kosakovsky Pong SL, Anderson CM, et al. Using HIV networks to inform real time prevention interventions. *PLoS One* **2014**; 9:e98443.
14. Dennis AM, Hue S, Learner E, Sebastian J, Miller WC, Eron JJ. Rising prevalence of non-B HIV-1 subtypes in North Carolina and evidence for local onward transmission. *Virus Evol* **2017**; 3:vex013.
15. Perez-Losada M, Castel AD, Lewis B, et al. Characterization of HIV diversity, phylodynamics and drug resistance in Washington, DC. *PLoS One* **2017**; 12:e0185644.
16. Volz EM, Ionides E, Romero-Severson EO, Brandt M-G, Mokotoff E, Koopman JS. HIV-1 transmission during early infection in men who have sex with men: a phylodynamic analysis. *PLoS Med* **2013**; 10:e1001568.
17. Centers for Disease Control and Prevention. HIV in the southern United States. 2016 CDC issue brief. <https://www.cdc.gov/hiv/pdf/policies/cdc-hiv-in-the-south-issue-brief.pdf>. Accessed 12 July 2016.
18. Cope AB, Powers KA, Kuruc JD, et al. Ongoing HIV transmission and the HIV care continuum in North Carolina. *PLoS One* **2015**; 10:e0127950.
19. North Carolina HIV/STD Surveillance Unit. HIV incidence estimate in North Carolina. **2016**. [http://epi.publichealth.nc.gov/cd/stds/figures/factsheet\\_HIV\\_incidence\\_2014.pdf](http://epi.publichealth.nc.gov/cd/stds/figures/factsheet_HIV_incidence_2014.pdf). Accessed 26 February 2017.
20. North Carolina HIV/STD Surveillance Unit. 2016 North Carolina HIV/STD/hepatitis surveillance report. [http://epi.publichealth.nc.gov/cd/stds/figures/std16rpt\\_rev3.pdf](http://epi.publichealth.nc.gov/cd/stds/figures/std16rpt_rev3.pdf). Accessed 12 December 2017.
21. Dennis AM, Hué S, Pasquale D, et al. HIV transmission patterns among immigrant Latinos illuminated by the integration of phylogenetic and migration data. *AIDS Res Hum Retroviruses* **2015**; 31:973–80.
22. Ratmann O, van Sighem A, Bezemer D, et al. Sources of HIV infection among men having sex with men and implications for prevention. *Sci Transl Med* **2016**; 8:320ra2.
23. Edgar RC. MUSCLE: multiple sequence alignment with high accuracy and high throughput. *Nucleic Acids Res* **2004**; 32:1792–7.
24. Liu TF, Shafer RW. Web resources for HIV type 1 genotypic-resistance test interpretation. *Clin Infect Dis* **2006**; 42:1608–18.
25. Bennett DE, Camacho RJ, Otelea D, et al. Drug resistance mutations for surveillance of transmitted HIV-1 drug-resistance: 2009 update. *PLoS One* **2009**; 4:e4724.
26. Struck D, Lawyer G, Ternes AM, Schmit JC, Bercoff DP. COMET: adaptive context-based modeling for ultrafast HIV-1 subtype identification. *Nucleic Acids Res* **2014**; 42:e144.
27. Price MN, Dehal PS, Arkin AP. FastTree: computing large minimum evolution trees with profiles instead of a distance matrix. *Mol Biol Evol* **2009**; 26:1641–50.
28. Ragonnet-Cronin M, Hodcroft E, Hue S, et al. Automated analysis of phylogenetic clusters. *BMC Bioinformatics* **2013**; 14:317.
29. Drummond AJ, Suchard MA, Xie D, Rambaut A. Bayesian phylogenetics with BEAUti and the BEAST 1.7. *Mol Biol Evol* **2012**; 29:1969–73.
30. Rambaut A, Drummond A. Tracer version 1.4. **2007**. <http://beast.bio.ed.ac.uk/Tracer>. Accessed 26 July 2015.
31. Bouckaert R, Heled J, Kühnert D, et al. BEAST 2: a software platform for Bayesian evolutionary analysis. *PLoS Comput Biol* **2014**; 10:e1003537.
32. Hue S, Pillay D, Clewley JP, Pybus OG. Genetic analysis reveals the complex structure of HIV-1 transmission within defined risk groups. *Proc Natl Acad Sci U S A* **2005**; 102:4425–9.
33. North Carolina HIV/STD Surveillance Unit. North Carolina HIV/STD epidemiologic profile 2013. **2015**. [http://epi.publichealth.nc.gov/cd/stds/figures/Epi\\_Profile\\_2013.pdf](http://epi.publichealth.nc.gov/cd/stds/figures/Epi_Profile_2013.pdf). Accessed 12 July 2016.
34. Oster AM, Wertheim JO, Hernandez AL, Ocfemia M, Saduvala N, Hall HI. Using molecular HIV surveillance data to understand transmission between subpopulations in the United States. *J Acquir Immune Defic Syndr* **2015**; 70:444–51.
35. Volz EM, Le Vu S, Ratmann O, et al. Molecular epidemiology of HIV-1 subtype B reveals heterogeneous transmission risk: implications for intervention and control. *J Infect Dis* **2018**; 217:1522–9.
36. Centers for Disease Control and Prevention. Detecting, investigating, and responding to HIV transmission clusters. **2018**. <https://www.cdc.gov/hiv/pdf/funding/announcements/ps18-1802/CDC-HIV-PS18-1802-AttachmentE-Detecting-Investigating-and-Responding-to-HIV-Transmission-Clusters.pdf>. Accessed 7 August 2018.
37. Oster AM, France AM, Mermin J. Molecular epidemiology and the transformation of HIV prevention. *JAMA* **2018**; 319:1657–8.